Size Manipulated Photoluminescence and Phosphorescence in $CaTiO_3:Pr^{3+}$ Nanoparticles

Xianmin Zhang,[†,‡] Jiahua Zhang,*[,†] Xia Zhang,[†] Meiyuan Wang,[†,‡] Haifeng Zhao,[†] Shaozhe Lu,[†] and Xiao-jun Wang*[,†,§]

Key Laboratory of Excited State Processes, Changchun Institute of Optics, Fine Mechanics, and Physics, Chinese Academy of Sciences, 16 Eastern South Lake Road, Changchun 130033, China, Graduate School of Chinese Academy of Sciences, Beijing, 100039, China, and Department of Physics, Georgia Southern University, Statesboro, Georgia 30460

Received: August 1, 2007; In Final Form: September 21, 2007

Red emitting nanophosphors of $CaTiO_3:Pr^{3+}$ with various particle sizes were prepared by sol−gel methods and structurally characterized by X-ray diffraction and field emission scanning electron microscopy. The fluorescent and phosphorescent properties of $CaTiO_3:Pr^{3+}$ nanoparticles as a function of particle sizes were investigated by using photoluminescence and photoluminescence excitation spectra as well as time decay patterns of fluorescence and phosphorescence. On the analysis of the longer lifetimes at 300 K as compared to that at 77 K and the appearance of maximal photoluminescence, the dependence of photoluminescence on phosphorescence is demonstrated. A very highly efficient phosphorescence recombination channel in the nanophosphor is proposed and discussed. This work provides a promising method to develop novel phosphors by manipulating the number of traps on the surface of nanophosphors through adjusting the particle size.

Introduction

Materials with persistent light emission after the cessation of excitation are called phosphorescent materials,[1,2] which have attracted considerable attention for various displays and signing applications as friendly environmental and energy economized materials.[3−6] The number and depth of traps play major roles in the initial intensity and persistent time in long lasting phosphors.[7] Conventionally, traps can be created by charge defects or incorporation with auxiliary activators into the host.[8−12] On the basis of these methods, some oxide persistent phosphors exhibiting a high brightness of blue and green phosphorescence with better chemical stability over sulfides are commercially available.[8,9] However, commercial red emitting oxide persistent phosphors with long persistence times have not been obtained yet. Recently, much work has been concentrated on the red emitting novel phosphors of Pr^{3+} doped $CaTiO_3$.[13−20] The red emission originates from the intra-4f $^1D_2-{}^3H_4$ transition of Pr^{3+} peaking at 615 nm, which is ideal as the red component for various color display technologies.[13−15] To improve its phosphorescent intensity and persistent time, some research has been performed by several groups.[21−23] Royce and Matsuda observed that the persistent time of red phosphorescence in $CaTiO_3:Pr^{3+}$ can reach 20 min by being co-doped with MgO or ZnO.[21] Jia et al. found that the traps of afterglow in $CaTiO_3:Pr^{3+}$ have the nature of electron traps, which may be associated with defects of Pr^{4+} and oxygen vacancies.[22] Recently, Haranath et al. reported the phosphorescent enhancement of $(Ca,Zn)TiO_3:Pr^{3+}$ by adding nanosized silica powder to passivate the surface of the host to minimize the concentration of the undesirable defects.[23] In our previous work,[24,25] the enhancement of fluorescent and phosphorescent intensities of $CaTiO_3:Pr^{3+}$ was realized by adding rare earth ions Ln^{3+} (Ln = La, Lu, Gd) in the phosphors to perform charge self-compensation to suppress Ca^{2+} and Ti^{4+} vacancies, consequently significantly increasing the fluorescence emission efficiency. However, at present, all these procedures cannot provide enough energy for phosphorescence in applications because the number of the traps in $CaTiO_3:Pr^{3+}$ phosphors is inadequate.

In recent years, much attention has been paid to the synthesis and characterization of nanomaterials due to their novel properties differing from bulk materials, such as electronics[26] and mechanics,[27] which mainly come from high surface-to-volume ratios in nanomaterials, as well as the quantum size effect. The high surface-to-volume ratio leads to the presence of numerous defects (dangling bonds, absorptions, and defect states) on the surface of nanomaterials. These surface defects are a major factor affecting the fluorescence efficiency of nanocrystalline phosphors, and the efficiency of conventional phosphors generally decreases due to quenching by surface defects.[28] However, the study of surface defects on phosphorescence efficiency is rare. The density of traps plays an essential role in the persistence of phosphorescence materials.[7] To improve the phosphorescence intensity and persistent time, the increase of density of traps in the host is needed. The surface defects perhaps act as traps beneficial for the generation of phosphorescence when they are adjusted in suitable depths. In the present work, the effect of surface defects with increasing particle size on fluorescence and phosphorescence was investigated. This provides a potential method to develop novel phosphors by manipulating the number of traps on the surface of nanophosphors through adjusting the particle size.

Experimental Procedures

A 0.01 M $CaCl_2$ and 0.01 M citric acid ethanol solution and $PrCl_3$ solution (Pr_6O_{11} was dissolved in HCl) were mixed. The molar ratio of Ca^{2+} to Pr^{3+} was 1:0.4%. Under constant magnetic stirring, $Ti(OC_4H_9)_4$ was slowly added until a yellow

* To whom correspondence should be addressed. E-mail: zjiahua@public.cc.jl.cn; tel.: +86-431-8670-8875.
† Changchun Institute of Optics, Fine Mechanics, and Physics.
‡ Graduate School of Chinese Academy of Sciences.
§ Georgia Southern University.

10.1021/jp076128l CCC: $37.00
Published on Web 11/20/2007 PAGE EST: 4.1

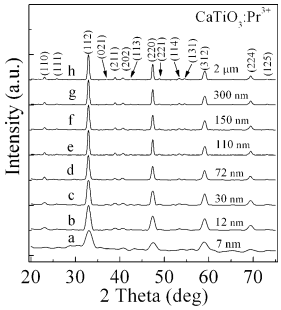

Figure 1. XRD patterns of $CaTiO_3:Pr^{3+}$ for nanoparticles at different sintering temperatures and bulk sample. The nanoparticles were prepared at (a) 450 °C, (b) 500 °C, (c) 600 °C, (d) 650 °C, (e) 750 °C, (f) 800 °C, and (g) 950 °C for 2 h and (h) bulk sample.

sol was obtained. By heating the yellow sol at 100 °C for 10 h, the sol changed to a gel. After further firing at 300 °C for 2 h, a dark solid mass was obtained. When it was cooled to room temperature, it was ground into a powder. White nanosized $CaTiO_3:Pr^{3+}$ particles with varying sizes were obtained after sintering the black powder at different temperatures for 2 h in air. Then, the nanoparticles were washed 2 times with distilled water and dried in an oven at 80 °C for 10 h. The bulk powder was synthesized by a conventional solid state reaction at 1400 °C for 3 h in air.[25]

The structural characterization was analyzed by X-ray diffraction (XRD; Rigaku D/max-rA) spectra with tahe Cu Kα line of 1.540 78 Å. The morphology of products was observed by field emission scanning electron microscopy (FESEM, Hitachi S-4800). Energy dispersive spectroscopy (EDS) was performed on a GENESIS2000XMS 60S (EDAX Inc). Photoluminescence (PL), PL excitation (PLE), and phosphorescence decay curves were measured using a Hitachi F-4500 fluorescence spectrophotometer. Fluorescence and phosphorescence were measured after irradiation by 365 nm ultraviolet (UV) light for 10 min. For lifetime measurements, the third (355 nm) harmonic of a Nd−YAG laser was used as the excitation source, and the signal was detected with a Tektronic digital oscilloscope mode TDS 3052.

Results and Discussion

Microstructure Character of the $CaTiO_3:Pr^{3+}$ Nanoparticles: XRD, FESEM, and EDS Studies. Figure 1 shows the XRD patterns of $CaTiO_3:Pr^{3+}$ nanoparticles with different sizes sintered at various temperatures as well as a bulk material. The phase of the bulk is orthorhombic (JCPDS Card No. 82−-0228). XRD patterns of nanoparticles are consistent with the bulk. Because of size effects, the peak of the nanoparticles was wider than that of the bulk.[29] By applying the Scherrer formula to the full width at half-maximum of the diffraction peaks, we calculated that the mean particle sizes of samples a−d were 7, 12, 30, and 72 nm, respectively, which is consistent with measurements determined by FESEM images of the nanoparticles, as shown in Figure 2. The analysis of chemical composition of $CaTiO_3:Pr^{3+}$ nanoparticles using EDS confirms the results of XRD on the phase composition and stoichiometry. A representative EDS spectrum is shown in Figure 3. The element ratio Ca/Ti/O = 20.37:20.64:58.98 was calculated from the EDS data and is very near to the standard ratio (1:1:3), further indicating that the nanoparticles are $CaTiO_3$. The dependence of particle size on sintering temperature is illustrated in Figure 4, indicating particle growth with an increase of temperature.

Size Effect on Photoluminescent Properties. PL and PLE spectra of $CaTiO_3:Pr^{3+}$ nanoparticles with different sizes are

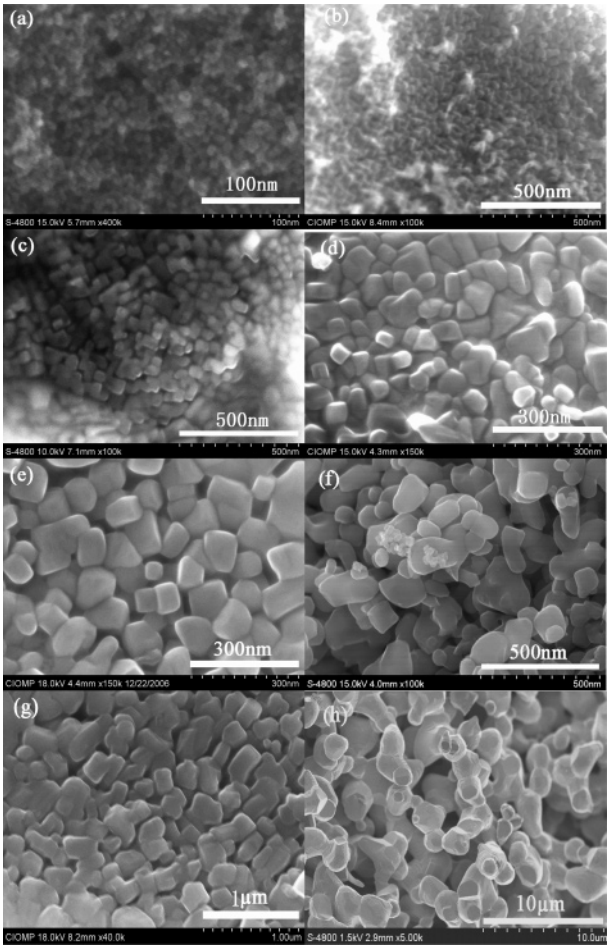

Figure 2. FESEM images of $CaTiO_3:Pr^{3+}$ nanoparticles at different sintering temperatures. The nanoparticles were prepared at (a) 450 °C, (b) 500 °C, (c) 600 °C, (d) 650 °C, (e) 750 °C, (f) 800 °C, and (g) 950 °C for 2 h and (h) bulk sample.

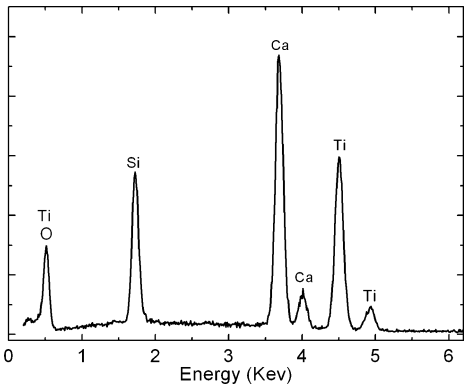

Figure 3. EDS analysis of $CaTiO_3:Pr^{3+}$ nanoparticles prepared at 600 °C.

presented in Figure 5, where the curve for bulk powders is also plotted for comparison. The PL spectra show a red emission line at 615 nm originating from the intra-4f $^1D_2-^3H_4$ transition of Pr^{3+}.[13] The PLE spectra monitoring the red emission mainly consists of two broad bands (A and B) in the UV region, which are located at 319 nm (A) and 265 nm (B), respectively. In comparison to the spectra of $CaTiO_3:Pr^{3+}$ bulk powders (dashed line), band A shifts from 330 nm in the bulk to 319 nm in the nanoparticles. The position of band A was experimentally observed to be consistent with that of the band edge absorption of the $CaTiO_3$ host due to O(2p)-Ti(3d) transition,[15] indicating that the blue shift of band A in the nanoparticles was the result

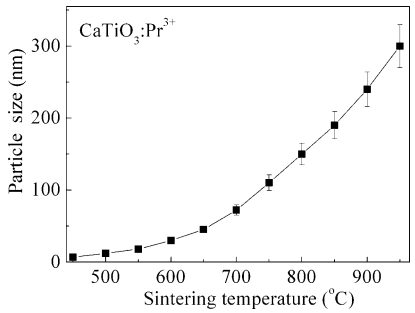

Figure 4. Dependence of particle sizes on sintering temperature.

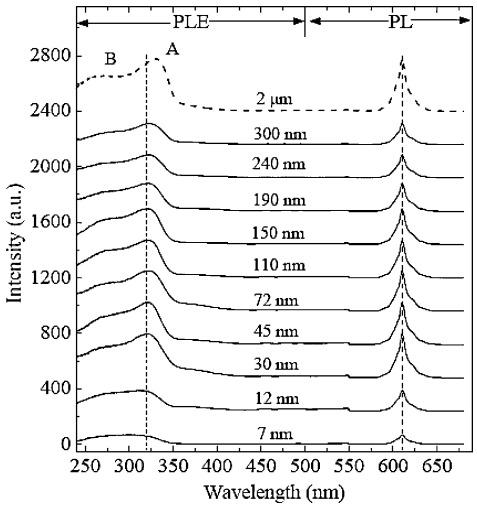

Figure 5. PL and PLE spectra of $CaTiO_3:Pr^{3+}$ nanoparticles with different sizes and bulk sample. PL was detected by being excited into the strong absorption band of the host with 319 nm for the nanoparticles and 330 nm for the bulk.

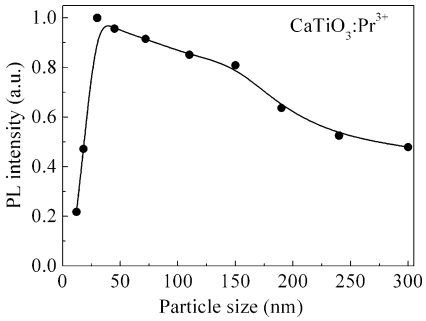

Figure 6. Dependence of fluorescence intensities of $CaTiO_3:Pr^{3+}$ on particle size.

of a size confinement effect, which was also observed in $CaTiO_3:Pr^{3+}$ thin films.[30] Band B exhibiting no obvious shift in the nanoparticles is attributed to the $4f^2 \rightarrow 4f5d$ absorption of Pr^{3+} ions.[15] As is shown in Figure 5, the PL intensities of the nanoparticles are lower than that of the bulk powders due to the existence of a large number of surface states on the surface of nanoparticles, which generally act as nonradiative centers to reduce luminescent efficiency.[28] Therefore, the enhancement of PL intensities with the increase of particle size is expected. However, it is found that the PL intensities of $CaTiO_3:Pr^{3+}$ nanoparticles reach a maximum at 30 nm, beyond which the PL intensities decrease, as shown in Figure 6. To understand the mechanism of PL intensity dependence on particle size, the lifetimes of the $^1D_2$ level of Pr^{3+} in $CaTiO_3$ nanoparticles with different sizes were measured at 300 and 77 K for comparison, as shown in Figure 7. It was found that the lifetimes at 77 K in all nanoparticles were shorter than that of the corresponding

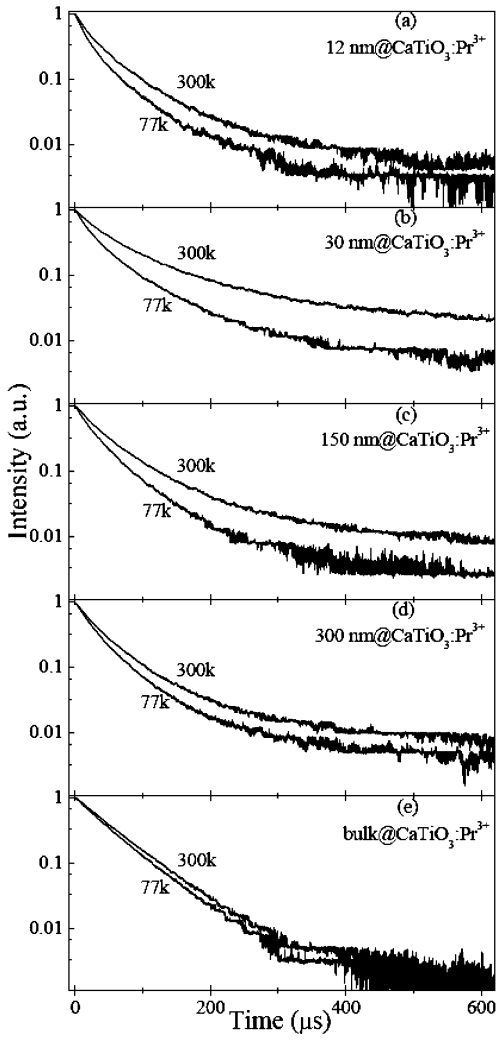

Figure 7. Fluorescence lifetime of Pr^{3+} ($^1D_2 - {}^3H_4$) in $CaTiO_3:Pr^{3+}$ nanoparticles with different particle sizes (12, 30, 150, and 300 nm) and bulk sample detected at 77 and 300 K, respectively.

samples at 300 K. This is different from the observation in other rare earth doped materials, in which the lifetimes of active centers increase due to the decrease of nonradiative relaxation at low temperatures.[31,32] In view of the observation of phosphorescence in $CaTiO_3:Pr^{3+}$ nanoparticles,[16,33] the longer lifetimes at 300 K are considered to be the result of the existence of a phosphorescent component originating from shallow surface traps in the PL, which can be shortened at 77 K because of the deficiency of thermal released energy. Therefore, the PL intensity measured at room temperature includes the phosphorescence originating from the shallow traps on the surface of $CaTiO_3:Pr^{3+}$ nanoparticles besides the fluorescence by directly exciting the $^1D_2 - {}^3H_4$ transition of Pr^{3+}.

As shown in Figure 7, the difference of the decay patterns between 77 and 300 K is the largest for 30 nm. This indicates that there exists the largest phosphorescent component in the PL of 30 nm $CaTiO_3:Pr^{3+}$ particles. The phosphorescence intensity is proportional to the trap number and transfer efficiency from filled trap to luminescent centers. On one hand, the surface of the nanoparticles can provide a large amount of traps besides some nonradiative recombination centers.[33] The traps reduce with increasing the particle size. On the other hand, the transfer efficiency from filled trap to luminescent centers is enhanced with increasing the particles because of the reduction of nonradiative recombination centers. As a result, the maximal phosphorescence intensity occurs at a specific size, which is

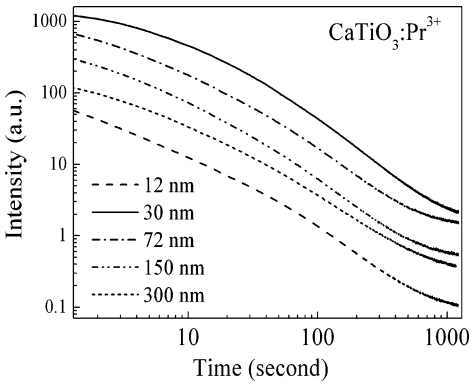

Figure 8. Phosphorescent decay curves of $CaTiO_3:Pr^{3+}$ for nanoparticles with different particle sizes (12, 30, 72, 150, and 300 nm) after irradiation by 365 nm UV light for 10 min.

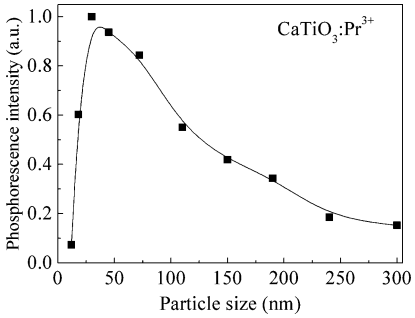

Figure 9. Dependence of phosphorescent intensities of $CaTiO_3:Pr^{3+}$ on particle size.

30 nm for $CaTiO_3:Pr^{3+}$ nanoparticles. Hence, the appearance of maximum PL intensity under room temperature is the contribution of phosphorescent components in PL. The lifetimes of the $^1D_2$ level of Pr^{3+} in the bulk sample were also measured for comparison, as shown in Figure 7e. It is found that the lifetimes at 77 K are nearly the same as that at 300 K and that the decay curves are linear. This indicates that there is no contribution of phosphorescent components in PL of bulk $CaTiO_3:Pr^{3+}$ and that the traps of bulk powders are different from those of nanoparticles. Jia et al. proposed that the traps of phosphorescence in bulk $CaTiO_3:Pr^{3+}$ had the nature of electron traps, which may be associated with defects of Pr^{4+} and oxygen vacancies.[22] The previous[33] and present work of our research group shows that the traps of phosphorescence in $CaTiO_3:Pr^{3+}$ nanoparticles mainly originate from surface defects.

However, the carriers for PL and phosphorescence emission conventionally recombine with the luminescence centers through conduction or valence bands. Thus, the total PL intensities including phosphorescent components should increase with the increase of particle size because the nonradiative recombination centers are reduced monotonically with particle enlargement. One has to consider that there exists another phosphorescent recombination channel that has a higher transfer efficiency than that of the recombination through the conduction band for an electron trap or the valence band for a hole trap. With this consideration, the phosphorescent component can dominate the PL.

Size Effect on Phosphorescent Properties. Figure 8 illustrates the time decay curves of phosphorescence in $CaTiO_3:Pr^{3+}$ with differently sized nanoparticles after irradiation with 365 nm UV light for 10 min. The largest integrated area under the decay curve is also shown for the 30 nm sample. The existence of the maximum in phosphorescence for a particle size had been discussed in the section of Size Effect on Photoluminescent Properties. Figure 9 shows the dependence of phosphorescence intensities on $CaTiO_3:Pr^{3+}$ particle sizes. In comparison with Figure 6, one can find that the phosphorescence attenuates faster than the PL as the particle size increases from 30 to 300 nm. This feature is the result of no fluorescent component in the phosphorescence. The pure fluorescence should be enhanced monotonically with increasing particle size due to the reduction of nonradiative recombination centers, which reduce the attenuation of PL intensity at particle sizes beyond 30 nm, as shown in Figure 6.

Conclusion

Red emitting phosphors of $CaTiO_3:Pr^{3+}$ with various particle sizes from 7 to 300 nm were prepared by sol−gel methods. Size manipulated photoluminescence and phosphorescence in the $CaTiO_3:Pr^{3+}$ nanoparticle was studied. The dependence of the photoluminescence on the phosphorescence was demonstrated. The maximal value of phosphorescence and photoluminescence intensities occurs at a size of 30 nm for $CaTiO_3:Pr^{3+}$ nanoparticles. It was also found that there exists a very highly efficient phosphorescence recombination channel that is higher than that of the recombination through the conduction band for an electron trap or the valence band for a hole trap. Thus, adjusting the number of traps on the surface of nanophosphors by manipulating the particle size provides a new method to develop novel phosphors.

Acknowledgment. This work was financially supported by the MOST of China (2006CB601104 and 2006AA03A138) and the National Natural Science Foundation of China (10574128).

References and Notes

(1) Blasse, G.; Grabmaier, B. C. *Luminescence Materials*; Springer-Verlag: Berlin, 1994.

(2) Shionoya, S.; Yen, W. M. *Phosphors Handbook*; CRC Press: Boca Raton, FL, 1999.

(3) Clabau, F.; Rocquefelte, X.; Jobic, S. T.; Deniard, P.; Whangbo, M. H.; Garcia, A.; Le Mercier, T. *Chem. Mater.* **2005**, *17*, 3904.

(4) Clabau, F.; Rocquefelte, X.; Le Mercier, T.; Deniard, P.; Jobic, S.; Whangbo, M. H. *Chem. Mater.* **2006**, *18*, 3212.

(5) Qiu, J. R.; Gaeta, A. L.; Hirao, K. *Chem. Phys. Lett.* **2001**, *333*, 236.

(6) Liu, Y. L.; Lei, B. F.; Shi, C. S. *Chem. Mater.* **2005**, *17*, 2108.

(7) Jia, D.; Meltzer, R. S.; Yen, W. M.; Jia, W.; Wang, X. *Appl. Phys. Lett.* **2002**, *80*, 1535.

(8) Matsuzawa, T.; Aoki, Y.; Takeuchi, N.; Murayama, Y. *J. Electrochem. Soc.* **1996**, *143*, 2670.

(9) Jia, W.; Yuan, H.; Lu, L.; Liu, H.; Yen, W. M. *J. Cryst. Growth* **1999**, *200*, 179.

(10) Jia, D.; Wang, X. J.; Yen, W. M. *Chem. Phys. Lett.* **2002**, *363*, 241.

(11) Lin, Y. H.; Tang, Z. L.; Zhang, Z. T.; Nan, C. W. *Appl. Phys. Lett.* **2002**, *81*, 996.

(12) Liu, B.; Shi, C. S.; Qin, Z. M. *Appl. Phys. Lett.* **2005**, *86*, 191111.

(13) Vecht, A.; Smith, D. W.; Chadha, S. S.; Gibbons, C. S. *J. Vac. Sci. Technol., B: Microelectron. Nanometer Struct.—Process., Meas., Phenom.* **1994**, *12*, 781.

(14) Cho, S. H.; Yoo, J. S.; Lee, J. D. *J. Electrochem. Soc.* **1996**, *143*, 231.

(15) Diallo, P. T.; Boutinaud, P.; Mahiou, R.; Cousseins, J. C. *Phys. Status Solidi A* **1997**, *160*, 255.

(16) Pan, Y. X.; Su, Q.; Xu, H. F.; Chen, T. H.; Ge, W. K.; Yang, C. L.; Wu, M. M. *J. Solid State Chem.* **2003**, *174*, 69.

(17) Wang, X. S.; Xu, C. N.; Yamada, H.; Nishikubo, K.; Zheng, X. G. *Adv. Mater.* **2005**, *17*, 1254.

(18) Kyomen, T.; Sakamoto, R.; Sakamoto, N.; Kunugi, S.; Itoh, M. *Chem. Mater.* **2005**, *17*, 3200.

(19) Yamamoto, H.; Okamoto, S.; Kobayashi, H. *J. Lumin.* **2002**, *100*, 325.

(20) Liu, X. M.; Jia, P. Y.; Lin, J.; Li, G. Z. *J. Appl. Phys.* **2006**, *99*, 124902.

(21) Royce, M. R.; Matsuda, S. U.S. Patent 5,656,094, 1997.

(22) Jia, W.; Jia, D.; Rodriguez, T.; Evans, D. R.; Meltzer, R. S.; Yen, W. M. *J. Lumin*. **2006**, *119*−*120*, 13.

(23) Haranath, D.; Khan, A. F.; Chander, H. *Appl. Phys. Lett*. **2006**, *89*, 91903.

(24) Zhang, X. M.; Zhang, J. H.; Zhang, X.; Chen, L.; Lu, S. Z. Wang, X. J. *J. Lumin*. **2007**, *122*−*123*, 958.

(25) Zhang, X. M.; Zhang, J. H.; Zhang, X.; Chen, L.; Luo, Y. S.; Wang, X. J. *Chem. Phys. Lett.* **2007**, *434*, 237.

(26) Lijima, S. *Nature (London, U.K.)* **1991**, *354*, 56.

(27) Ball, P.; Garwin, L. *Nature (London, U.K.)* **1992**, *355*, 761.

(28) Tissue, B. M. *Chem. Mater.* **1998**, *10*, 2837.

(29) Wei, Z. G.; Sun, L. D.; Liao, C. S.; Yin, J. L.; Jiang, X. C.; Yan, C. H. *J. Phys. Chem. B* **2002**, *106*, 10610.

(30) Boutinaud, P.; Tomasella, E.; Ennajdaoui, A.; Mahiou, R. *Thin Solid Films* **2006**, *515*, 2316.

(31) Manoj Kumar, G.; Narayana Rao, D.; Agarwal, G. S. *Phys. Rev. Lett*. **2003**, *91*, 203903.

(32) Chen, X. Y.; Zhuang, H. Z.; Liu, G. K.; Li, S.; Niedbala, R. S. *J. Appl. Phys.* **2003**, *94*, 5559.

(33) Zhang, X. M.; Zhang, J. H.; Nie, Z. G.; Wang, M. Y.; Ren, X. G.; Wang, X. J. *Appl. Phys. Lett*. **2007**, *90*, 151911.